PCCP

Accepted Manuscript

ROYAL SOCIETY OF CHEMISTRY

www.rsc.org/pccp

Physical insights into salicylic acid release from poly(anhydrides)

Queeny Dasgupta[1], Kaushik Chatterjee [1,2], Giridhar Madras[1,3*]

[1]Centre for Biosystems Science and Engineering, [2]Department of Materials Engineering and

[3]Department of Chemical Engineering,

Indian Institute of Science, Bangalore-560012, India

[*]Corresponding author +91-80-2293 2321; giridhar@chemeng.iisc.ernet.in

Abstract

Salicylic acid (SA) based biodegradable polyanhydrides (PAHs) are of great interest for drug delivery in a variety of diseases and disorders owing to the multi-utility of SA. There is a need for designing SA-based PAHs for tunable drug release optimal for different needs. In this work, we have devised a simple strategy for tuning the release properties and erosion kinetics of a family of PAHs. PAHs incorporating SA were derived from related aliphatic diacids, varying only in the chain length and prepared by simple melt condensation polymerization. Upon hydrolysis induced erosion, the polymer degrades into cytocompatible products including the incorporated bioactive SA and the diacid. The degradation follows first order kinetics with the rate constant varying nearly 25 times between the PAH obtained with adipic acid and dodecanedioic acid. The release profiles have been tailored from 100 % to 50 % SA release in 7 days across the different PAHs. The release rate constants of these semi-crystalline, surface eroding PAHs decreased almost linearly with an increase in the diacid chain length. The release rate constants varied by nearly 40 times between the adipic acid and dodecanedioic acid PAH. The degradation products with SA concentration in a range of 30-350 ppm were used to assess cytocompatibility and showed no cytotoxicity to HeLa cells. This particular strategy is expected to: (a) enable synthesis of application specific PAHs with tunable erosion and release profiles; (b) encompass a large number of drugs that may be incorporated in the PAH matrix. Such a strategy can potentially be extended to the controlled release of other drugs that may be incorporated in the PAH backbone and has important implications for the rational design of drug eluting bioactive polymers.

Keywords: controlled release; biodegradable polymers; antibacterial; tunable erosion.

Introduction

Poly(anhydrides) (PAHs) are a versatile class of polymeric biomaterials that have found extensive use in biomedical applications, particularly in the area of drug delivery.[1-3] These polymers are best suited for short term drug release.[4, 5] Controlled release of several drugs has been successfully achieved by loading drugs in PAHs.[6, 7] These polymers are typically hydrophobic but they possess hydrolytically labile anhydride linkages. The presence of these linkages qualifies these materials as prospective biodegradable materials. The major benefit of PAHs is that these are typically composed of diacid precursors. Because these precursors are often endogenous to the human body, PAHs do not elicit inflammatory responses when used as biomaterial implants.[8, 9]

A variety of PAH structures has been synthesized and evaluated to accomplish application specific drug release behavior. Apart from changing the nature/ structure of the polymeric backbone to aliphatic or aromatic, combinations of the two have also been tried.[10, 11] PAHs like poly(maleic anhydride) have been synthesized such that anhydride linkages are present in the pendant side chains instead of the primary backbone.[12, 13] Owing to the diverse requirements of stimuli-responsiveness[14] in drug release applications, it is important to understand the correlation between the structure of the polymer and its subsequent influence on physical properties such as degradation and drug release.[15]

Aliphatic PAHs have created significant interest in the area of short term drug release particularly because of their simple diacid constitution. They are semi-crystalline in nature and typically have melting temperatures higher than the physiological temperature.[16] These are commonly synthesized by simple solvent-free melt polycondensation techniques and may,

therefore, be considered safe for biomedical applications. Since PAHs come under the class of insoluble, hydrophobic polymers, degradation or mass loss involves an inevitable step of erosion (as a consequence of polymer chain scission). For such hydrolytic chain scission to occur, the bonds present in the vicinity of the cleavable bonds also play a pivotal role. A more hydrophobic chemical structure present in the proximity of the anhydride bond will allow lesser water retention and, subsequently, slower degradation than a hydrophilic structure.

The influence of linker structure on release from PAH backbone has been studied earlier[17]. However, a systematic study of the degradation and release properties of a family of SA based PAHs has not been conducted. In the present work, we use a particular strategy of varying the chain length of the diacid to understand its influence on the degradation/ erosion kinetics and on the SA release behavior. This study thus provides a systematic comparison of SA-loaded polyanhydrides that offers new physical insights into changes that occur in physico-chemical, degradation and release properties resulting from the differences in chain length of the reactant. We believe that these physical insights can facilitate the rational design of SA loaded polymers for drug delivery.

SA is a potent drug used for its antibacterial,[18, 19] anti-inflammatory,[20, 21] anti-pyretic, anti-cancerous[22] applications etc. However, their dosages vary significantly depending on the intended application. The time course of release is also an important characteristic that determines its suitability for an application. These anhydrides are of particular interest in drug delivery because they undergo surface erosion and are most suitable for providing controlled release. The anti-inflammatory and anti-microbial effects of SA are well reported and the immediate release of SA from these anhydrides could help mitigate these issues. The only parameter varied in these PAHs is the diacid such as adipic acid, suberic acid, sebacic acid and

dodecanedioic acid. These are linear, aliphatic diacids that have monotonically increasing chain lengths.

2. EXPERIMENTAL

2.1 Materials

Diacyl chlorides, adipoyl chloride (AC, Sigma Aldrich), suberoyl chloride (SC, Sigma Aldrich), sebacoyl chloride (SeC, TCI chemicals, India), and dodecanedioyl chloride (DC, Sigma Aldrich) were used. Acetic anhydride (AAn) was procured from Sigma Aldrich. Salicylic acid (SA) was obtained from SD Fine Chemicals, India. Solvents used at various stages of the work include ethyl acetate (EtoAc), chloroform, dichloromethane (DCM), dimethylsulfoxide (DMSO) and N,N-dimethylformamide (DMF), acetone (all from Merck, India).

2.2 Synthesis

Step I: ***Synthesis of SA based diacids***

SA (1 mol. equiv. 7 g, 50.7 mmol) was dissolved completely in THF (10 mL). Pyridine (2 mol. equiv., 8.3 mL, 101.4 mmol) was added and allowed to stir in this solution for 15 min at 35 ˚C. The respective diacyl chlorides (0.5 mol. equiv.) were added slowly at 0 ˚C (ice bath) to the stirred solution. The ice bath was removed after addition and the reaction mixture was stirred for 12 to 16 h at 37 ˚C. After completion of the reaction, hydrochloric acid was added to the reaction mixture kept at 0 ˚C (ice bath) to precipitate the diacid. Acid was added until a pH of 2 was reached. The obtained precipitate (white) was washed repeatedly with water. The precipitate was then vacuum filtered and dried to constant weight before further reaction with anhydride in the next step. This step was based on a previously reported work.[23]

Step II: ***Synthesis of acetylated diacids***

5 g of the synthesized diacid was placed in a round bottomed flask with excess AAn (50 mL) at 160 ˚C under reflux conditions for 2.5 h. After this, the excess AAn was removed from the system at 85 ˚C under vacuum. The obtained precipitate are dissolved in THF and then precipitated by pouring this solution drop-wise to stirred petroleum ether at 4 ˚C. The activated diacids are now acetylated.

Step III: ***Polymerization of acetylated diacid***

The anhydride precursors were polymerized by a simple melt condensation process. The precursors obtained in the previous step were melted at 160 ˚C and stirred under N_2 atmosphere and vacuum (60 mm Hg) for ~1 h. The obtained polymer was dissolved in THF and dried in rotary evaporator at 37 ˚C. The synthesis scheme is detailed in Scheme 1. The resulting PAHs were named P4ASA, P6ASA, P8ASA and P10ASA, respectively where the numbers indicate the number of methylene units in the respective diacids, PA indicate **p**oly(**a**nhydrides) and SA indicates **s**alicylic **a**cid.

The loading concentrations of SA as obtained by dissolving polymer discs in PBS (pH 9.0) are 4.6, 3.5, 2.6 and 1.9 (% by weight) for P4ASA, P6ASA, P8ASA and P10ASA, respectively.

2.3 Materials characterization

2.3.1 FTIR spectroscopy

The synthesized PAHs were chemically characterized by FTIR spectroscopy. Spectra were recorded on a Perkin-Elmer Frontier FT-NIR/MIR spectrometer under universal attenuated total reflectance (uATR-FTIR) mode. The recording range extended from 4000-650 $cm^{-1}$and the spectrum was an average of 32 scans with a resolution of 4 cm^{-1}.

2.3.2 ^{1}H NMR spectroscopy

Proton-nuclear magnetic resonance (NMR) spectroscopy was also used for chemical characterization. The spectra were recorded on a 400 MHz Bruker Avance NMR spectrometer. 2 mg of the prepolymer was dissolved in 500 µL of $CDCl_3$ (for P4ASA and P6ASA) and d6-DMSO (for P8ASA and P10ASA) with 0.03 % (v/v) tetramethylsilane as internal reference (Deutero, Germany).

2.3.3 Molecular weight determination

The molecular- weight distribution (MWD) was obtained by gel permeation chromatography (GPC, Waters, Milford, USA). The setup was maintained at 50°C and consisted of an isocratic pump, three size-exclusion columns (Waters Styragel HR 4, HR 3, and HR 0.5 columns (300 × 7.5 mm)), a differential refractive index detector (Waters, R415) and data acquisition system. The eluent used in the system was THF and run at a flow rate of 0.9 mL/min. were used. Samples were injected in a Rheodyne valve with a 100 µL sample loop. The chromatograph was converted to MWD using the universal calibration with polystyrene

standards (Polymer Lab, Poole, UK). The Mark-Houwink constants were obtained from previously reported literature.[24]

2.3.3 Differential scanning calorimetry

Synthesized PAHs were thermally characterized on a differential scanning calorimeter (DSC, TA Instruments, Q2000). PAH samples weighing 5-7 mg were placed in a copper pan and crimped. The samples were then exposed to a uniform temperature program from –50 to 200 ˚C with a temperature ramp of 5 ˚C/ min.

2.3.4 Surface water wettability

The wettabilities of the samples were analyzed by measuring the water contact angle with a contact angle goniometer (Dataphysics). The static contact angles were evaluated by placing a 1 μL droplet of ultrapure water (Sartorius) on polymer discs (10 mm in diameter). The contact angle was measured after the drop equilibrated ~10 s after it was placed. The data is represented as mean ±standard deviation (S.D) based on three independent measurements.

2.3.5 Hydrolytic degradation studies

The samples were melted and made into discs of 5 mm diameter. These samples were then placed in 20 mL phosphate buffered saline (PBS) of pH 7.4. The samples were maintained at 37 ˚C in an incubator shaker maintained under shaking conditions (100 rpm). The samples are removed from PBS at specified time points and weighed after drying to constant weight in a vacuum desiccator. The mass loss of the polymer was measured using the following formula:

$$\%\, \boldsymbol{weight\ loss} = \frac{\boldsymbol{M_o - M_t}}{\boldsymbol{M_o}} \times \mathbf{100} \qquad \textbf{(1)}$$

In equation (1), M_o and M_t indicate the initial and final weights of the PAH discs, respectively. All samples were made in triplicate and the mass loss data are represented as mean $\pm$ standard deviation.

2.3.6 SA release studies

SA release from the PAH matrices was evaluated to compare the release kinetics of the different polymers. Discs, as prepared for degradation studies were immersed in 20 mL PBS at 37 ˚C and 100 rpm and allowed to degrade over time. The release media was collected and the UV spectrum was recorded in a UV-vis spectrophotometer (Shimadzu, UV-1700 PharmaSpec).SA has characteristic absorption maxima at 297 nm. The SA concentration was determined by comparing with the standard calibration curve.

2.3.7 Cytocompatibility studies

HeLa, a cervical carcinoma cell line was used for assessing the cytocompatibility of the PAHs. HeLa cells- are a sturdy cell line classified as a standard cell line for evaluation of cytocompatibility of biomedical polymers. The cells were cultured in Dulbecco's modified Eagle's medium (DMEM, Gibco, Life Technologies) supplemented with 10 % (v/v) fetal bovine serum (FBS, Gibco, Life Technologies) and antibiotics (1 % (v/v) penicillin-streptomycin). The cells were given growth conditions of 37 ˚C and 5% CO_2. This study used cells of Passage 13. Cytocompatibility was estimated using an indirect method where cells were treated with conditioned media. Conditioned media were prepared by immersing 5 mm discs (thickness 1 mm) of P4ASA, P6ASA, P8ASA and P10ASA and allowed to undergo hydrolytic degradation for 24 h in 5 mL complete media (DMEM+FBS). HeLa cells were exposed to this pre-conditioned media and allowed to grow in its presence. Cell viability was monitored at specific

time points of 1 day and 3 days. The initial cell seeding density was 5000 cells/ well in a 48-well plate. The cells were first allowed to attach to wells for 6 h (in the presence of fresh medium). The fresh medium was then replaced with 500 µL/ well of conditioned media. This study used fresh medium as the control. Both fresh and conditioned media (both fresh and conditioned) were replenished after every 24 h during the course of the study.

After treatment in conditioned media, cell viability was estimated using MTT (3-(4,5-Dimethylthiazol-2-yl)-2,5-Diphenyltetrazolium Bromide, Sigma Aldrich) assay. The respiratory chain reduces MTT and other tetrazolium salts by the action of oxidoreductases produced by live cells. A stock solution of 5 mg/mL of MTT was made initially. The working solution was a diluted solution of 1 mg/mL. For the cell proliferation assay, 200 µL of MTT solution (1 mg/mL) was added to each well. The well plates were kept unperturbed at 37 ˚C in 5% CO_2 for 3 h. Water insoluble formazan crystals were solubilized in DMSO and its absorbance was measured at 570 nm in a well plate reader (Synergy HT, Biotek). The absorbance value is proportional to the number of mitochondria in the well. The mean of absorbance values from five independent wells was obtained to give the final absorbance. The data are represented as mean ± S.D. for n=5. Analysis of variance (ANOVA) with Tukey's test was used for all statistical analysis and significances were considered significant for $p<0.05$.

2.3.8 Anti-bacterial activity

To assess the pharmacological activity of the drug released from the PAHs, the effectiveness of the polymers were evaluated against *S. aureus* (ATCC 25923).Luria Bertani (LB) broth medium was used to culture *S. aureus*. Bacteria were allowed to grow overnight in an incubator shaker (100 rpm) and maintained at a temperature of 37 ˚C. The overnight culture

(200 μL) was added to 5 mL of fresh LB medium and grown for 2 h. PAHs were dispersed in the LB medium (3 mg/mL) and the bacterial cultures were added to obtain a final optical density of 0.1 at 600 nm (OD_{600}). Bacterial growth was monitored by obtaining OD_{600} at 6 h and 24 h after initial incubation. The readings from the replicates are reported as mean ± S.D. for n= 3.

3. RESULTS AND DISCUSSION

The synthesized PAHs have molecular weights ranging from 8300-49000 Da (as shown in Table 1) with a polydispersity index of 1.4. The molecular weights increased as the chain length of the diacid precursor increases.

3.1 FTIR spectroscopy

All the acids (AC, SC, SeC and DC) show the characteristic IR peak at 1690 cm^{-1} due to the –C=O stretching of the carboxylic chloride. After the synthesis of the diacid in the first step, a peak appears at the 1750 cm^{-1}indicating the formation of the ester bond at the –OH group of SA. The peak at 1690 $cm^{-1}$is still present indicating the presence of the free –COOH group. After the reaction with AAn and subsequent polymerization under vacuum, two peaks are observed in FTIR. The peaks at 1815 cm^{-1} and 1740 cm^{-1} indicate the formation of anhydride bond. The anhydride bond shows two characteristic –C=O stretching vibrations and is, therefore, characterized by two peaks (Figure 1). All peaks match previously reported literature.[25]

3.2 NMR spectroscopy

NMR spectroscopy (Figure S1, see electronic supplementary information) confirms the chemical characterization as observed in FTIR. All peaks in the ^1H NMR spectra match previously reported data in literature.[26, 27] ^1H NMR confirms the presence of all the peaks corresponding to protons in the $–CH_2$ (methylene) units of the diacids. The peaks from the di-

carboxylic acids are displayed in the range between 0.8-2.4 ppm. The peaks of the monomers match those obtained in the polyesters. More shielded $–CH_2$ groups are present as the chain length of the di-carboxylic acid increases.P4ASA contains protons only attached to α, β carbons; whereas P10ASA contains protons attached to α, β, γ, δ and ε carbons. This confirms the structure of the PAHs. However, the formation of the anhydride is confirmed by the ^{13}C NMR that confirms the presence of a peak at 170 ppm corresponding to the carbon of the anhydride bond. This is present for all the synthesized PAHs.

3.3 Differential scanning calorimetry

Thermal characterization (Figure S2, see electronic supplementary information) of the four PAHs shows that the melting temperature (T_m) increases as the chain length of the diacid increases. The T_m values obtained are 53, 57, 66 and 85 ˚C for P4ASA, P6ASA, P8ASA and P10ASA, respectively. The longer hydrophobic chains of DC as compared to AC cause the substantial increase of the T_m from 53 to 85 ˚C. There is a considerable increase in the crystallization temperature (T_c) as the chain length increases. The T_c is 40, 42, 56 and 74 ˚C for P4ASA, P6ASA, P8ASA and P10ASA, respectively. Correspondingly, the T_g ranges from –27 to –3 ˚C and scales with the diacid chain length. The increase in T_g may be attributed to the higher degree of polymerization in the higher chain length PAH as compared to their shorter chain counterparts (as shown in Table 1). The longer chain restricts the rotational flexibility of the polymer chains, thereby, causing an increase in the T_g. However, since all the synthesized PAHs have T_g lower (and T_m higher) than the physiological temperature (37 ˚C), this family of PAHs is suitable for biomedical applications. The ends of a polymer chain have more freedom of motion as compared to the inner segments. Low molecular weight polymers have more chain ends per unit volume and, therefore, higher free volume and lower T_g.

The crystallization temperature (T_c) also increases as the chain length of the diacid increases. T_c values range from 40 to 74 ˚C between the 4 PAHs and increase as a function of the diacid chain length. The degree of crystallinity may be calculated by considering the area under the crystallization curve and is the enthalpy of crystallization (ΔH). It is observed that the crystallinity increases as the chain length of the diacid increases. The ΔH values obtained are 38, 48, 92 and 132 J/g for P4ASA, P6ASA, P8ASA and P10ASA, respectively. The increase in crystallinity is generally accompanied with a concomitant increase in the T_m, as observed in this family of PAHs.

PAHs with higher loading concentration of SA (~15 %) were synthesized and it was observed that these polymers had T_m values very close to 37 ˚C. This is undesirable as drug delivery is considerably affected if $T_m \leq 37$ ˚C. Therefore, all further synthesis and characterization were performed on PAHs with loading < 5 %.

3.4 Surface water wettability

The surface water wettability pertains to the hydrophobicity of the polymeric material. The hydrophobicity increases in the following trend: P4ASA< P6ASA< P8ASA< P10ASA. The values of the water contact angles are tabulated in Table 1. The increase in the contact angle and subsequent decrease in the wettability may be attributed to the number of methylene ($-CH_2$) units present in the parent diacid. Longer aliphatic chains are more hydrophobic than their shorter counterparts. The increased hydrophilicity may also be attributed to the higher loading % of SA in the shorter chain diacids than their longer chain counterparts. SA is hydrophilic and its higher inclusion in the matrix leads to increased hydrophilicity of the PAH.

3.4 Hydrolytic degradation studies

The hydrolytic degradation rate increases as the chain length decreases and follows: P4ASA>P6ASA>P8ASA>P10ASA. P4ASA, P6ASA, P8ASA and P10ASA degrade 100, 90, 50 and 28 % in 48 h, respectively (Figure 2a). The degradation data show that the PAHs degrade between 30-100 % in the first 48 h of hydrolysis. This fast degradation may limit their uses in biomedical applications. However, the need for antimicrobial, anti-inflammatory drugs is most often immediate after an implantation. The incorporated SA is reported to possess both of these features and may, therefore, be considered suitable for therapeutic applications.

The higher hydrophobic chains of the longer chain acids allow lesser water permeation than the shorter chain diacids. The solubility of adipic acid in water is considerably higher than that of the other diacids.[28] The hydrolytically labile anhydride bonds are located in the proximity of the aliphatic chains. As shown in the contact angle studies, the hydrophobicity of these chains increases with the diacid chain length. Owing to this, the water available at the vicinity of the anhydride bond decreases as the chain length increases. Lesser water results in lower hydrolysis of the anhydride bonds and, consequently, lower mass loss.

- Hydrolytic degradation causes chain scission in the backbone of the polymer due to bulk or surface erosion.[29, 30] In most cases it occurs as a simultaneous bulk or surface phenomenon, where one mechanism is more predominant. The anhydride bonds are extremely labile to hydrolysis, and thus the degradation of the surface anhydrides takes place much faster than its penetration into the bulk of the matrix.[31] Since the mass loss due to degradation is accompanied by a concomitant decrease in the sample dimensions, it is likely that the erosion takes place layer

by layer from the surface of the matrix.[29] This is further corroborated by the kinetics of mass loss, as discussed below.

3.5 Kinetics of degradation

The degradation kinetics of these PAHs may be modelled using the following equation:

$$-\frac{dM}{dt} = kM^n \qquad (2)$$

In equation 2, k is the degradation rate constant and n is the order of degradation. First order release kinetics is followed in all four PAHs as is evident by fitting the degradation data to the following equation:

$$\ln(\frac{M_t}{M_0}) = -kt \qquad (3)$$

In equation 3, M_t and M_o are final and initial weights of the polymer at time t and time t=0, respectively. A semi-log plot of $\frac{M_0}{M_t}$ with time was linearly regressed to obtain the degradation rate constant (Figure 2b). The values of k ($\times 10^{-3} h^{-1}$) obtained are 120, 45, 11.9 and 4.5 for P4ASA, P6ASA, P8ASA and P10ASA, respectively. The value of k increases by an order of magnitude for P4ASA as compared to P8ASA and similarly, for P6ASA compared to P10ASA.

3.6 SA release studies

SA release was evaluated by monitoring the SA concentration in the release media. It is observed that the release follows: P4ASA>P6ASA>P8ASA>P10ASA. In the first 48 h, the polymers P4ASA, P6ASA, P8ASA and P10ASA release 98, 80, 34 and 12 %, respectively (Figure 2c). The fast SA release observed in P4ASA and P6ASA may be attributed to two factors: (i) the lesser hydrophobic nature of AC and SC as compared to SeC and DC; (ii) the

complete degradation of the P4ASA and P6ASA in 48 h and 96 h, respectively. Another major factor driving the release of SA from these polymeric matrices is because these aliphatic PAHs are generally hydrophobic in nature.[29] Thus, there is a tendency of the hydrophilic SA to be released in the media.

3.7 Kinetics of release

The kinetics of release follow the first order degradation of the PAH matrices. The SA release may be modeled using the following equation,

$$-\frac{dC}{dt} = k_r C^n \qquad (4)$$

In equation 4, C is the concentration of the drug remaining in the polymer, k_r is the release rate constant and n is order of release. Considering first order release and integrating equation 4,

$$\ln\left(\frac{C_t}{C_0}\right) = -k_r t \qquad (5)$$

In equation 5, C_0 and C_t are the initial and final SA concentrations at time t=0 and t=t, respectively. The semi-log plot of C_t/C_0 with time shows that the k_r ($\times 10^{-3} h^{-1}$) values obtained are 94, 40, 9.9 and 2.2 for P4ASA, P6ASA, P8ASA and P10ASA, respectively (Figure 2d). The release rates are consistent with the degradation data and show that release rate constant increases with decrease in the diacid chain length. Thus, k_r/k is nearly the same for P4ASA, P6ASA and P8ASA indicating that release and degradation are related. Similar to the degradation rates, the rate constant of release is nearly an order of magnitude higher for P4ASA as compared to P8ASA. Higher hydrophobicity of P8ASA compared to P4ASA (Table 1) allows lesser water in their vicinity,[32, 33] thereby hindering the degradation and consequently, the release

from the PAH matrix. Thus, the degradation of the polymer plays a key role in determining the amount of drug released from the matrix.

3.8 Cytocompatibility studies

The cell studies showed that cell proliferation was not affected by the degradation products of the PAHs. In spite of the decreased pH of the medium due to the fast degradation of P4ASA and P6ASA, the conditioned media were not toxic to the cells. P4ASA, P6ASA, P8ASA and P10ASA release 350 ppm, 100 ppm, 40 ppm and 25 ppm, respectively in 24 h. This concentration is estimated as per the release profiles of SA in PBS. Release concentrations may differ slightly in complete culture medium. Release concentration could not be obtained directly from the medium because of the interference of serum proteins at the emission maximum of SA (297 nm). The MTT assay (Figure 3) showed comparable cell viability in the conditioned media treated cells to that of the control (fresh medium treated). The cell numbers increased congruously, as monitored after 1 day and 3 days. The cells appear to be well spread across all samples and establish good cell to cell contact in 3 days (Figure 4). There was no statistically significant difference observed across the samples.

3.9 Antibacterial studies

The antibacterial studies of the PAHs show that all four PAHs are active against *S. aureus.* This study also shows that the released SA is pharmacologically active. The polymers did not show any significant difference from the blank (untreated) after 6 h. However, after 24 h of growth in the presence of the PAHs, the PAHs show a significant drop in the OD_{600} value indicating much lesser bacterial growth. All the PAHs showed similar antibacterial effect. In order to find significant differences between the polymers, paired t-test with p=0.05 was

conducted and it is observed that P4ASA and P10ASA show significantly different antibacterial activities (Figure 5). This difference may be due to the appreciable disparity in the amount of SA released between the two polymers. P4ASA and P10ASA release 350 and 25 ppm, respectively in 24 h. This higher release of SA from P4ASA may be attributed to its higher activity against *S. aureus*. P4ASA shows ~72 % decrease in bacterial count as compared to the control (blank untreated sample).

4. Conclusions

We have successfully synthesized a family of PAHs for SA delivery. We have investigated in detail their degradation and drug release kinetics by varying the chain length of the precursor diacid. The chain length of the precursor plays an important role in controlling the rate of drug release from the polymeric system and may, therefore, be effectively used as a strategy to tailor drug release from aliphatic PAHs for application specific purposes. The released drug showed pharmacological activity against bacterial cells. Owing to their cytocompatibility, these SA-based polymers may find uses for biomedical applications.

5. Acknowledgements

The authors are grateful to the Department of Biotechnology (DBT), India (BT/PR5977/MED/32/242/2012) for providing financial support for this work. G.M. thanks the Department of Science and Technology (DST), India for J. C. Bose fellowship. K.C. acknowledges the Ramanujan fellowship from DST. The authors wish to thank the NMR research centre, IISc Bangalore for providing access to the NMR facility.

References

1. H. B. Rosen, J. Chang, G. Wnek, R. Linhardt and R. Langer, *Biomaterials*, 1983, **4**, 131-133.
2. K. Leong, B. Brott and R. Langer, *J. Biomed. Mater. Res.*, 1985, **19**, 941-955.
3. W. Khan, V. G. S. Challa, R. Langer and A. J. Domb, in *Focal Controlled Drug Delivery*, Springer, 2014, pp. 3-32.
4. B. D. Ulery, H. M. Kan, B. A. Williams, B. Narasimhan, K. W. H. Lo, L. S. Nair and C. T. Laurencin, *Adv. Healthc. Mater.*, 2014, **3**, 843-847.
5. S. Ponnurangam, G. D. O'Connell, C. T. Hung and P. Somasundaran, *Colloids Surf., B*, 2015.
6. J. P. Jain, S. Modi, A. Domb and N. Kumar, *J. Controlled Release*, 2005, **103**, 541-563.
7. J. Wang, G. Yang, X. Guo, Z. Tang, Z. Zhong and S. Zhou, *Biomaterials*, 2014, **35**, 3080-3090.
8. J. E. Vela-Ramirez, J. T. Goodman, P. M. Boggiatto, R. Roychoudhury, N. L. Pohl, J. M. Hostetter, M. J. Wannemuehler and B. Narasimhan, *The AAPS journal*, 2015, **17**, 256-267.
9. S. S. Snyder, T. J. Anastasiou and K. E. Uhrich, *Polym. Degrad. Stab.*, 2015, **115**, 70-76.
10. E. Shen, M. J. Kipper, B. Dziadul, M.-K. Lim and B. Narasimhan, *J. Controlled Release*, 2002, **82**, 115-125.
11. D. Teomim and A. J. Domb, *Biomacromolecules*, 2001, **2**, 37-44.
12. I. Donati, A. Gamini, A. Vetere, C. Campa and S. Paoletti, *Biomacromolecules*, 2002, **3**, 805-812.
13. M. Maniar, X. Xie and A. J. Domb, *Biomaterials*, 1990, **11**, 690-694.

14. S. G. Roy, K. Bauri, S. Pal, A. Goswami, G. Madras and P. De, *Polym. Int.*, 2013, **62**, 463-473.

15. A. Göpferich and R. S. Langer, *J. Polym. Sci., Part A: Polym. Chem.*, 1993, **31**, 2445-2458.

16. H. R. Kricheldorf and Z. Gomourachvili, *Macromol. Chem. Phys.*, 1997, **198**, 3149-3160.

17. A. Prudencio, R. C. Schmeltzer and K. E. Uhrich, *Macromolecules*, 2005, **38**, 6895-6901.

18. N. D. Stebbins, M. A. Ouimet and K. E. Uhrich, *Adv. Drug Deliv. Rev.*, 2014, **78**, 77-87.

19. L. Rosenberg, A. Carbone, U. Römling, K. Uhrich and M. Chikindas, *Lett. Appl. Microbiol.*, 2008, **46**, 593-599.

20. C. Banti, A. Giannoulis, N. Kourkoumelis, A. Owczarzak, M. Kubicki and S. Hadjikakou, *J. Inorg. Biochem.*, 2015, **142**, 132-144.

21. R. Amann and B. A. Peskar, *Eur. J. Pharmacol.*, 2002, **447**, 1-9.

22. E. Bastiaannet, K. Sampieri, O. Dekkers, A. de Craen, M. van Herk-Sukel, V. Lemmens, C. van den Broek, J. W. Coebergh, R. Herings and C. van de Velde, *Brit. J. cancer*, 2012, **106**, 1564-1570.

23. Y. Chandorkar, R. K. Bhagat, G. Madras and B. Basu, *Biomacromolecules*, 2014, **15**, 863-875.

24. E. Ron, E. Mathiowitz, G. Mathiowitz, A. Domb and R. Langer, *Macromolecules*, 1991, **24**, 2278-2282.

25. J. P. Coates, *Appl. Spectrosc. Rev.*, 1996, **31**, 179-192.

26. B. M. Vogel and S. K. Mallapragada, *Biomaterials*, 2005, **26**, 721-728.

27. E. Mathiowitz, E. Ron, G. Mathiowitz, C. Amato and R. Langer, *Macromolecules*, 1990, **23**, 3212-3218.

28. E. C. Attané and T. F. Doumani, *Ind. Eng. Chem.*, 1949, **41**, 2015-2017.

29. A. Göpferich and J. Teßmar, *Adv. Drug Deliv. Rev.*, 2002, **54**, 911-931.

30. A. Göpferich, *Biomaterials*, 1996, **17**, 103-114.

31. S. Domanskyi, K. L. Poetz, D. A. Shipp and V. Privman, *PCCP*, 2015, **17**, 13215-13222.

32. Q. Dasgupta, K. Chatterjee and G. Madras, *Biomacromolecules*, 2014, **15**, 4302-4313.

33. J. Yu, F. Lin, P. Lin, Y. Gao and M. L. Becker, *Macromolecules*, 2013, **47**, 121-129.

Table 1: Physical properties of PAHs

Polyester	M_w (Da)	T_g (˚C)[a]	T_m(˚C)[a]	T_c(˚C)[a]	ΔH (J/g)	Contact angle (°)[b]	Mass loss (%) in 7 days[c]	Degradation rate constant, k× 10^{-3} (h^{-1})	SA release (%) in 7 days[c]	Release rate constant, $k_r \times 10^{-3}$ (h^{-1})
P4ASA	**8300**	**-27**	**53**	**40**	**38**	**32**	**100**	**120**	**100**	**94**
P6ASA	**10200**	**-21**	**57**	**43**	**48**	**56**	**100**	**45**	**100**	**40**
P8ASA	**13300**	**-5**	**66**	**57**	**92**	**68**	**85**	**11.9**	**84**	**9.9**
P10ASA	**49000**	**-3**	**84**	**64**	**132**	**82**	**57**	**4.5**	**28**	**2.2**

[a] Within a range of $\pm$ 2 ˚C

[b] Within a range of $\pm$ 2 ˚

[c] Error $\pm$1

Figure Captions

Scheme 1: Synthesis scheme of SA incorporated PAHs (P4ASA). The diacyl chlorides were changed to result in different PAHs.

Figure 1: FTIR spectra of the PAHs.

Figure 2: Variation of (a) $\frac{M_t}{M_0}$ and (b) $\ln(\frac{M_0}{M_t})$ with hydrolytic degradation time and variation of (c) $\frac{C_t}{C_\infty}$ and (d) $\ln(\frac{C_0}{C_t})$ with release time for P4ASA, P6ASA, P8ASA and P10ASA. The degradation rate constant and the release rate constant are obtained from the regressed lines in (b) and (d), respectively.

Figure 3: Cell viability assay (MTT data) of P4ASA, P6ASA, P8ASA and P10ASA based on absorbance at 570 nm.

Figure 4: Cell spreading on P4ASA after (a) 6 h, (b) 24 h and (c) 72 h.

Figure 5: Antibacterial activity of the PAHs.

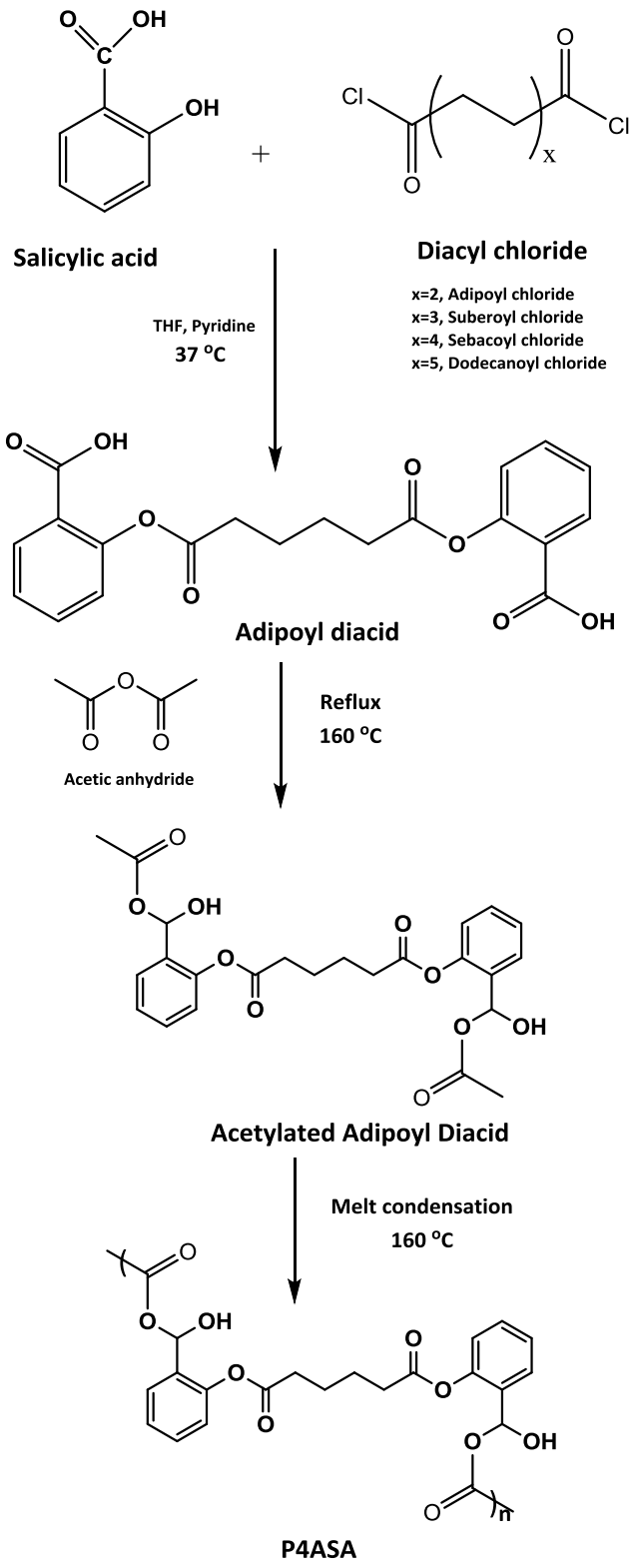

Scheme 1

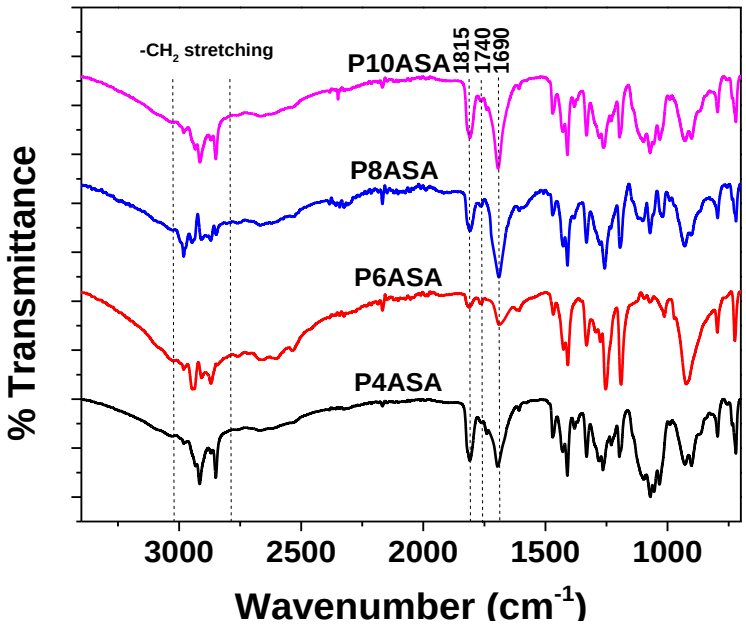

Figure 1

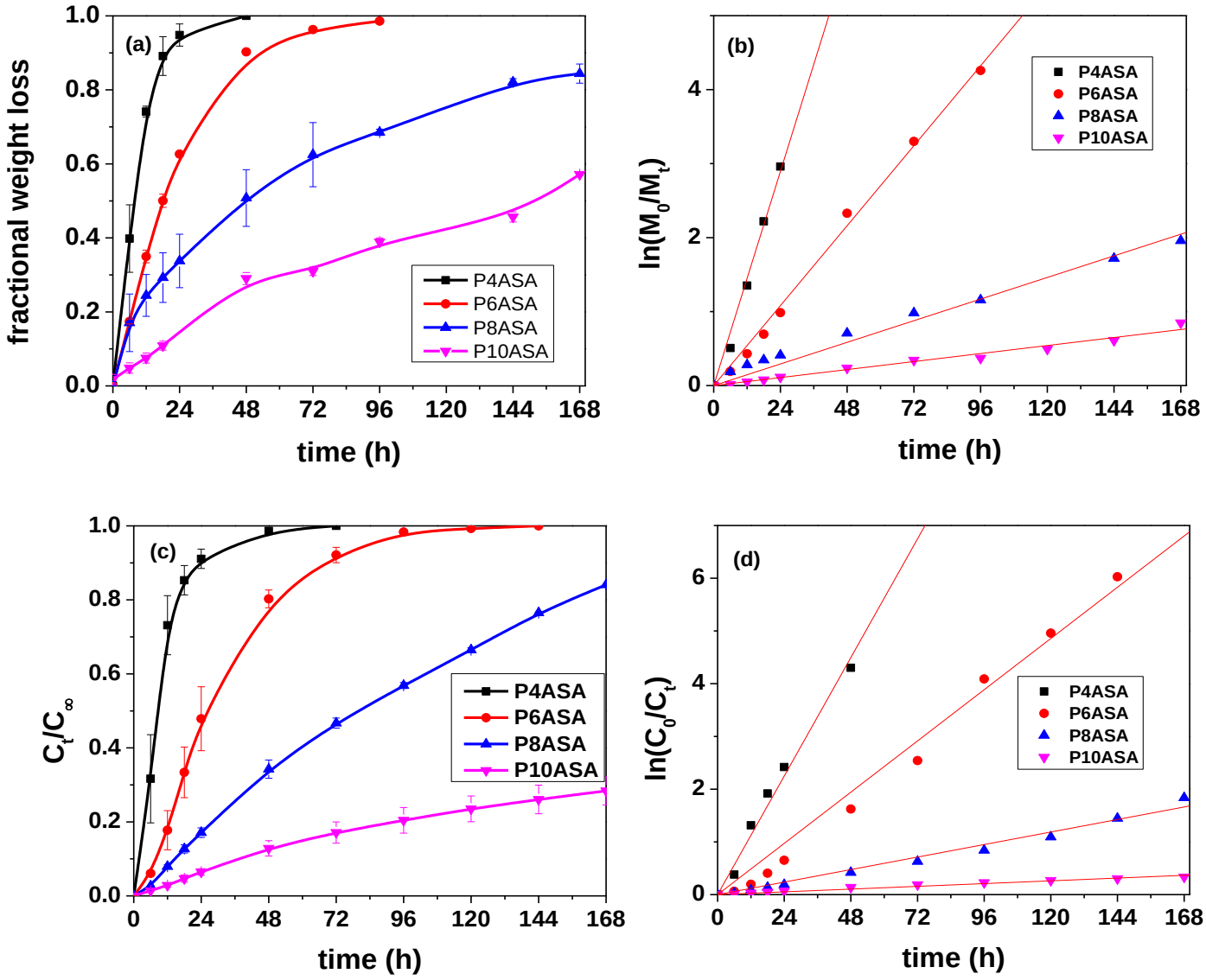

Figure 2

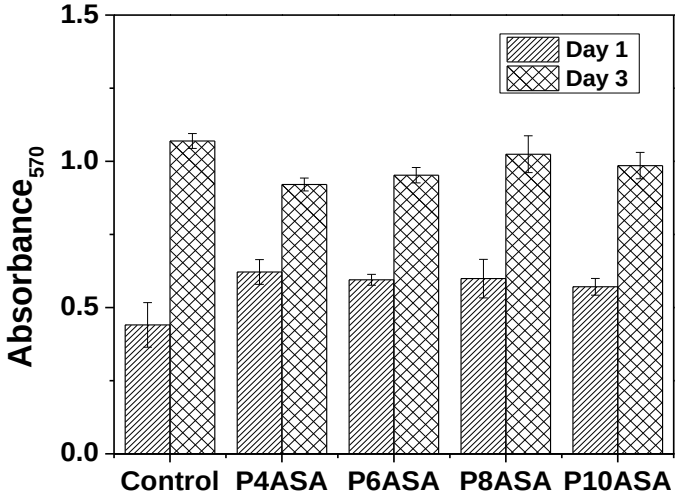

Figure 3

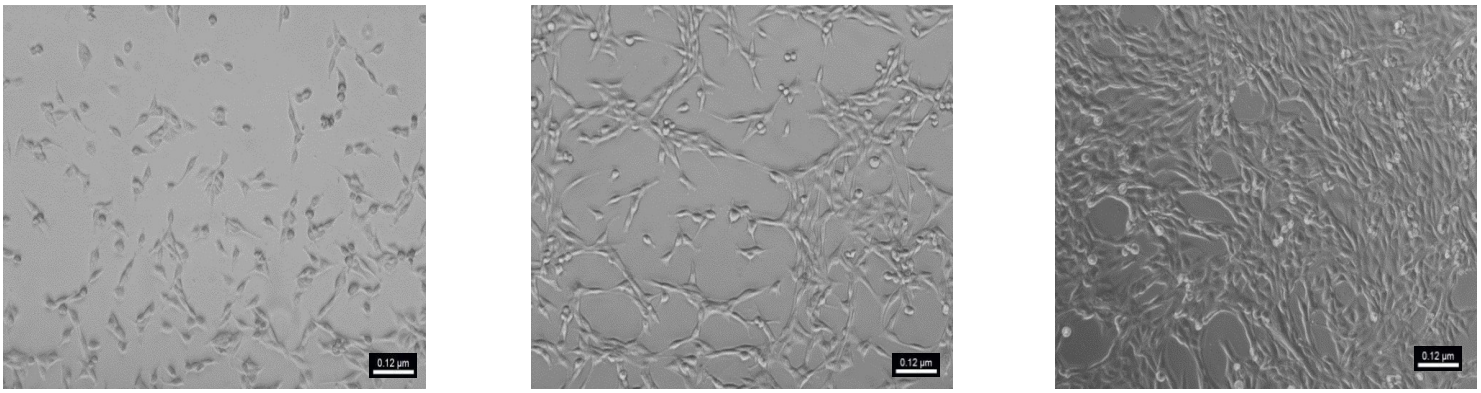

Figure 4

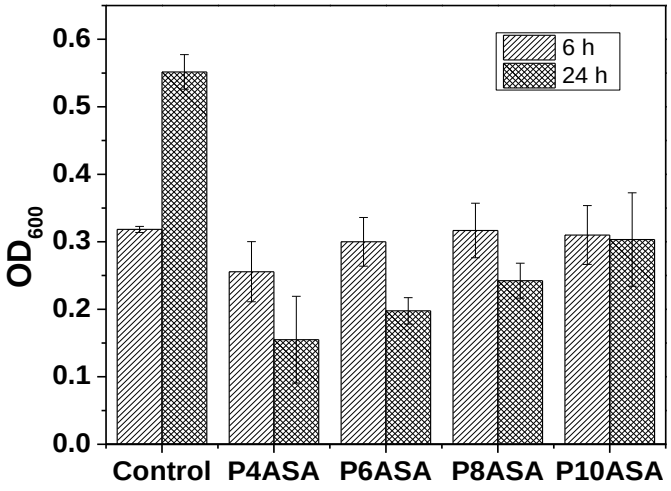

Figure 5